

No stellar age gradient inside supergiant shell LMC 4[★]

Jochen M. Braun¹, Dominik J. Bomans^{2,1,★★}, Jean-Marie Will^{1,***}, and Klaas S. de Boer¹

¹ Sternwarte der Universität Bonn, Auf dem Hügel 71, D-53121 Bonn, Germany

² University of Illinois at Urbana-Champaign, Department of Astronomy, 1002 West Green Street, Urbana, IL 61801, USA

Received 2 May 1997 / Accepted 21 July 1997

Abstract. The youngest stellar populations of a 'J'-shaped region inside the supergiant shell (SGS) LMC 4 have been analysed with CCD photometry in B , V passbands. This region consists of 2 coherent strips, one from the east to the west reaching about 400 pc across the OB superassociation LH 77 and another extending about 850 pc from south to north.

The standard photometric methods yield 25 colour-magnitude diagrams (CMDs) which were used for age determination of the youngest star population by isochrone fitting. The resultant ages lie in the range from 9 Myr to 16 Myr without correlation with the distance to the LMC 4 centre. We therefore conclude that there must have been one triggering event for star formation inside this great LMC SGS with a diameter of 1.4 kpc.

We construct the luminosity function and the mass function of five regions consisting of 5 fields to ensure that projection effects don't mask the results. The slopes lie in the expected range ($\gamma \in [0.22; 0.41]$ and $\Gamma \in [-1.3; -2.4]$ respectively). The greatest values of the slope occur in the north, which is caused by the absence of a young, number-dominating star population.

We have calculated the rate with which supernovae (SNe) have exploded in LMC 4, based on the finding that all stars are essentially coeval. A total of $5\text{--}7 \cdot 10^3$ supernovae has dumped the energy of $10^{54.5}$ erg over the past 10 Myr into LMC 4, in fact enough to tear the original star-forming cloud apart in the time span between 5 and 8 Myr after the starformation burst. We conclude that LMC 4 can have been formed without a contribution from stochastic self-propagating star formation (SSPSF), although the ring of young associations and H II regions around the edge have been triggered by the events inside LMC 4.

Key words: stars: early-type – Hertzsprung-Russell (HR) diagram – stars: luminosity function, mass function – ISM: bubbles – ISM: individual objects: LMC 4 – Magellanic Clouds

Send offprint requests to: J.M. Braun ('jbraun@astro.uni-bonn.de')

[★] Based on observations collected at the European Southern Observatory (ESO), La Silla, Chile.

^{★★} Feodor Lynen-Fellow of the Alexander von Humboldt-Foundation

^{***} Present address: Hewlett-Packard GmbH, Herrenberger Str. 130, D-71034 Böblingen

1. Introduction

In the Magellanic Clouds (MCs) giant loops of H II regions can be recognized in deep pictures taken in $H\alpha$ light. These H II structures were divided by Goudis & Meaburn (1978) into two distinct groups: shell structures called giant shells (GSs) with diameters of 20–260 pc and the huge supergiant shells (SGSs) with diameters of 600–1 400 pc. Employing unsharp masking techniques and high contrast copying of the long exposed $H\alpha$ images of Davies et al. (1976, hereafter DEM), Meaburn and collaborators (see Meaburn 1980) subsequently identified 85 GSs and 9 SGSs in the Large Magellanic Cloud (LMC) and 1 SGS in the Small Magellanic Cloud (SMC).

Unlike GSs whose structure can be explained by the combined activity of supernova explosions, stellar winds and radiation pressure of the central star association(s), SGSs (i.e. structures about 1 kpc in diameter) need very effective, gigantic mechanisms for their creation. Such large scale features, which rival in size only with spiral structures, might be created, according to the appraisal of mechanisms by Tenorio-Tagle & Bodenheimer (1988), by the collision of high velocity clouds (HVCs) with the disk of the galaxy or by stochastic self-propagating star formation (SSPSF).

The infall of an HVC would cause a well defined velocity deviating from the velocity of the original disk gas. Also, because of the short time scale of such a collision, an almost identical age is expected for all stars whose formation was triggered by that event.

In the case of SSPSF (see Feitzinger et al. 1981) star formation propagates from one point (e.g. the centre of a SGS) in all directions (e.g. towards the rim of a SGS). Thus one should see in projection two velocity components in the H I layer (a receding and an approaching component) as well as a clear age gradient of the star populations inside a SGS.

However, the observation of a central area of a SGS with little gas (i.e. a 'hole' in the H I layer) and of an approximately 200 pc thick shell of neutral material, which is ionized at the inner edge (visible as $H\alpha$ filaments) by the radiation from the associations containing numerous early type stars (see Lucke & Hodge 1970; Lucke 1974) in the centre of the SGS, would be consistent with both scenarios.

The importance of understanding the formation and the structure of SGSs is evident if one realizes how big they are. They may dominate large portions of a galaxy, in particular of the smaller irregular galaxies, such as the Magellanic Clouds are. Knowledge about the creation of SGSs leads to a better knowledge of the more recent development of the MCs and of their youngest star populations.

The shape and size of LMC 4 is such, that SSPSF has been considered as the most likely explanation for the formation of this SGS (see Dopita et al. 1985). However, observations of star groups along the edge of LMC 4 showed that the ages of these groups were of the same order as the time needed to create the SGS in the case of SSPSF (see Vallenari et al. 1993; Petr et al. 1994).

Reid et al. (1987) found from V , I photometry of Shapley Constellation III (the southern half of the SGS LMC 4, McKibben Nail & Shapley 1953) no clear age gradient, also inconsistent with a global SSPSF model.

Furthermore, Domgörgen et al. (1995) presented an investigation of LMC 4 based on H I data and IUE spectra. One result is that there is only one distinct velocity component towards us with 10 km s^{-1} and just a diffuse rear component. This is not consistent with an undisturbed expanding shell, but it indicates a break-out of the SGS at the back side of the LMC.

So LMC 4 resembles a cylinder rather than a sphere which should be expected in a galaxy with an H I scale height well below 500 pc. We note, however, that it is notoriously difficult to derive depth structure in a reliable way.

All these points show that we still do not well understand the history of LMC 4. To improve this situation, photometry of star groups *inside* LMC 4 was taken in 1993 with the goal to derive ages. This paper presents that data and the results. Additionally the star formation history is further investigated in Sect. 4 by looking for overlapping age groups in the derived mass functions.

2. Observations and data reduction

Our data¹ were taken in April, 1993 (during 13 nights in Dutch time) with the 0.91 m Dutch telescope (1st dataset). A second, very limited dataset was taken on the 6th February, 1996 with the 1.54 m Danish telescope.

The Dutch telescope was equipped with a 512^2 pix^2 Tektronix CCD (ESO #33) with a scale factor of $0.443'' \text{ pix}^{-1}$ (1 pix = $27 \mu\text{m}$) and a total field of view of $3.8' \times 3.8'$, the Danish telescope with a 2048^2 pix^2 Loral/Lesser CCD (W11-4 Chip) with a scale factor of $0.39'' \text{ pix}^{-1}$ (1 pix = $15 \mu\text{m}$).

The 1st dataset contains 25 CCD fields (0–24, see Fig. 3) with an overlap of about 80 pix. They form two coherent strips, one 400 pc strip through the OB superassociation LH 77 from east to west with 10 fields (i.e. CCD positions which cover an

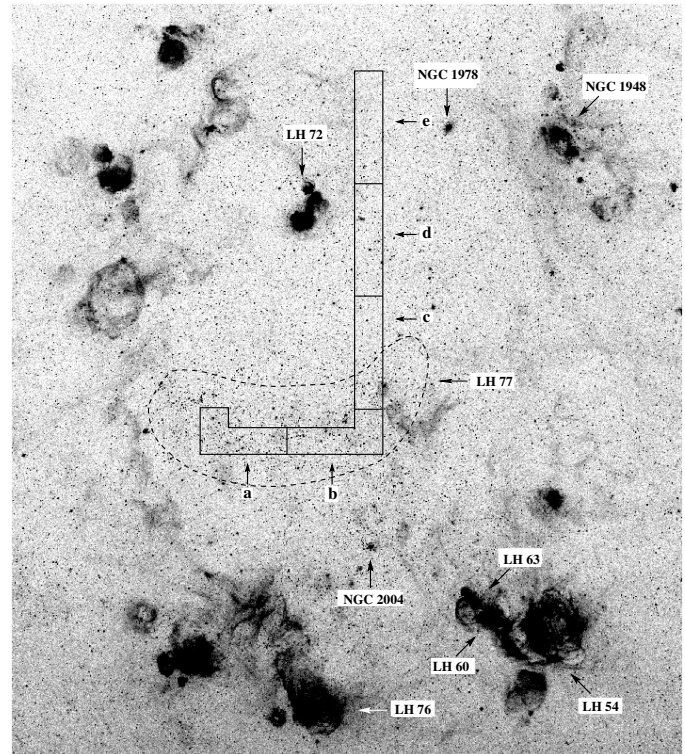


Fig. 1. $H\alpha$ image of supergiant shell LMC 4 made from a scan of a photographic plate taken with the Curtis Schmidt telescope at Cerro Tololo (Kennicutt & Hodge 1986). The locations of the important objects indicated in the text and of the 5 regions of the 1st dataset (named a–e, see Sect. 4) are marked

area of $14.2 \text{ } \square'$ each) and an 850 pc strip from the south to the north with 15 fields, reaching the rim of the supergiant shell LMC 4 (see Figs. 1 and 3). The whole 'J'-shaped area is about $298 \text{ } \square' = 0.083 \text{ } \square^\circ$ in size (without the 16% of overlapping regions). For each position we have long exposed frames of 10 min in the B and 5 min in the V passband (ESO #419 and #420) reaching down to approximately $V = 20$ mag (fields 0–4 corresponding to region a, see Sect. 4) or to $V = 21$ mag (fields 5–24 corresponding to regions b–e) and short exposed frames of 1 min in B and 0.5 min in V , all with a seeing of $1.3''$ – $2.6''$. The 2nd dataset contains 3 CCD fields (+0, +2 and +24, see Fig. 3) at the beginning and the end of the area covered by the 1st dataset. This set was obtained to get a better calibration of the main dataset, so we took short exposed frames in the B and V passbands (ESO #450 and #451) reaching down to $V = 19$ mag with a seeing of $1.8''$ – $2.7''$.

The data reduction was carried out with MIDAS and the built-in photometry package DAOPHOT II of Stetson (1987). Additionally some special steps (e.g. correction of bad double columns and reading the time information of the header) was done with IRAF.

To calibrate the frames we used the following standard fields of Landolt (1992): Rubin 149, PG 0918+029 and PG 1633+099. Because of wrong time information in the file headers we were only able to use the standard fields of night 8 and 9 of the

¹ The entire Tables 1 and 3 of this publication are only available electronically, at the CDS (see Editorial in A&A 280, E1, 1993) or at the Astronomical Institutes of Bonn University ('ftp ftp.astro.uni-bonn.de', see URL 'http://www.astro.uni-bonn.de/~jbraun/diploma.html' in the WWW for further information).

Table 1. Part of the table of photometric results around Sk $-67\ 198 = \text{MACS J0534}-670\#003$ (Magellanic Catalogue of Stars: Tucholke et al. 1996, see Table 3). The position of the stars in the (rough) general coordinate system (\tilde{x}, \tilde{y}) and on the long exposed B frames (x, y) are given with the calibrated B, V magnitudes and total errors (statistic and systematic) and the dereddened M_V and $(B - V)_0$ values. The table with 20 812 stars is available electronically (see the footnote to Sect. 2)

Field sequence number	\tilde{x} [pix]	\tilde{y} [pix]	x [pix]	y [pix]	V [mag]	ΔV [mag]	$B - V$ [mag]	$\Delta(B - V)$ [mag]	M_V [mag]	$(B - V)_0$ [mag]
\vdots	\vdots	\vdots	\vdots	\vdots	\vdots	\vdots	\vdots	\vdots	\vdots	\vdots
2.0030	678.1	437.7	340.9	266.8	16.145	0.074	-0.153	0.116	-2.696	-0.263
2.0031	853.4	441.3	165.7	270.4	16.130	0.075	1.697	0.119	-2.711	1.587
2.0032	757.4	450.6	261.6	279.7	11.866	0.073	0.000	0.116	-6.975	-0.110
2.0033	732.9	453.7	286.2	282.8	17.990	0.079	0.918	0.130	-0.852	0.808
2.0035	799.3	458.3	219.7	287.4	16.559	0.074	-0.143	0.116	-2.282	-0.253
\vdots	\vdots	\vdots	\vdots	\vdots	\vdots	\vdots	\vdots	\vdots	\vdots	\vdots

Table 2. Mean total and statistical errors with standard deviation of stellar V magnitudes and $B - V$ colours. The number of stars in the corresponding magnitude range is given in parentheses

Magnitude range [mag]	Mean errors [mag]	
	ΔV	$\Delta(B - V)$
(Number of stars)		
$V < 18$ (3 270)	0.076 (14) 0.014 (19)	0.120 (22) 0.021 (28)
$18 \leq V < 20$ (10 459)	0.090 (31) 0.045 (39)	0.144 (46) 0.068 (55)
$20 \leq V$ (7 083)	0.137 (63) 0.112 (70)	0.223 (100) 0.167 (101)

1st dataset (i.e. fields 11–16) and to calibrate the beginning (i.e. fields 0–3) and the end (i.e. fields 23–24) of the 'J'-shaped region by the 2nd dataset. To get a homogeneous dataset (see Table 1) we adjusted the magnitude levels of the fields 4–10 and 17–22 by their overlapping areas.

The calibration of the 1st dataset was done with the following equations:

$$V = V_n - 3.210(13) \text{ mag} + 0.029(7). \quad (1)$$

$$[(B - V)_n - 0.450(18) \text{ mag}]$$

$$(B - V) = [(B - V)_n - 0.450(18) \text{ mag}] / 0.907(9) \quad (2)$$

with index n indicating the normalization to exposure time 1 s and airmass 0 and of the shift from point spread function (PSF) to aperture magnitudes. The airmass correction was made by means of the atmospheric extinction coefficients measured on La Silla by the Geneva group (Burki et al. 1995a, b).

The mean errors of our photometry are given in Table 2. The total error contains all statistical and systematic errors (including PSF fit, calibration and PSF to aperture shift as their main part) and is rather an overestimation (see Fig. 2), while the statistical error from DAOPHOT is a clear overestimation of the reached accuracy.

There is no CCD photometry inside LMC 4 in the literature overlapping with our data, so we compared the brightest stars

of spectral type B0 to A9 and luminosity class I/Ia marked by Sanduleak (1969) with the B, V magnitudes of Rousseau et al. (1978). This leads to an unexpected high deviation of the 1st dataset, which concerns only up to five of the brightest (evolved) stars of a CCD field, so it won't effect the results of the isochrone fit. For all other stars the values of the 1st and 2nd dataset agree within the scope of the errors.

To calculate absolute magnitudes we used the distance modulus of $(m - M)_0 = 18.5$ mag (see Westerlund 1990, and refs. therein) corresponding to a distance of 50 kpc.

For identification purpose we looked for stars having MACS entries (Magellanic Catalogue of Stars) to get good positions; e.g. Sk $-67\ 198$ (Sanduleak 1969) equals MACS J0534-670#003 (de Boer et al. 1995; Tucholke et al. 1996) with the coordinates (2000): RA: $5^{\text{h}}\ 34^{\text{m}}\ 03.094^{\text{s}}$ and Dec: $-67^{\circ}\ 00'\ 59.24''$ (see Fig. 3 and Table 3).

Examples of the resulting colour-magnitude diagrams (CMDs) are shown in Fig. 2.

3. Determination of the age

We now proceed and will fit isochrones by eye to the colour-magnitude diagram of each field separately, with $\log(t/[\text{yr}])$ and E_{B-V} as fit parameters. We used the isochrones of the Geneva group (Schaerer et al. 1993) for LMC metallicity ($Z = 0.008$ or $[\text{Fe}/\text{H}] = -0.34$ dex). These isochrones include the effect of convective core overshooting and are based on the new opacities. The use of the isochrones of the Padova group (Alongi et al. 1993) would lead to slightly younger ages (about 0.05 in logarithmic age); but we stuck to the Geneva data to stay consistent with the analyses of other regions in and around LMC 4 by Olsen et al. (1997), Petr (1994) and Wilcots et al. (1996), as discussed in Sect. 5 (see Table 6). In all, we estimate that the accuracy of the determined ages is ~ 0.1 in logarithmic units.

According to Ratnatunga & Bahcall (1985) the number of foreground stars is negligible in respect of the fit. Thus one can expect about 3 stars of our Galaxy towards the LMC in the colour range of $B - V < 0.8$ mag and in the apparent visual magnitude range of $13 \text{ mag} < V < 19 \text{ mag}$ (corresponding to the abso-

Table 3. Cross identification of the stars in our analysed area with the MACS (Magellanic Catalogue of Stars: Tucholke et al. 1996), which may serve as an astrometric reference grid. As an example we give the data of 5 stars around Sk $-67\ 198 = \text{MACS J0534-670\#003}$. The field sequence number gives the CCD field (here 2) and the sequence number in the original DAOPHOT table, the x and y coordinates show the position on the long exposed B frames. The entire table is available electronically (see the footnote to Sect. 2)

MACS name	α [^h ^m ^s]	δ [^o ' "]	Field sequence number	x [pix]	y [pix]
⋮	⋮	⋮	⋮	⋮	⋮
J0533-669#053	5 33 59.941	-66 59 56.69	2.0202	216.1	412 .6
J0534-670#002	5 34 02.625	-67 00 32.02	2.0175	254.6	338 .9
J0534-670#003	5 34 03.094	-67 00 59.24	2.0032	261.6	279 .7
J0534-670#004	5 34 03.522	-67 01 49.54	2.0117	273.7	170 .4
J0534-670#005	5 34 04.026	-67 00 10.46	2.0047	269.8	386 .5
⋮	⋮	⋮	⋮	⋮	⋮

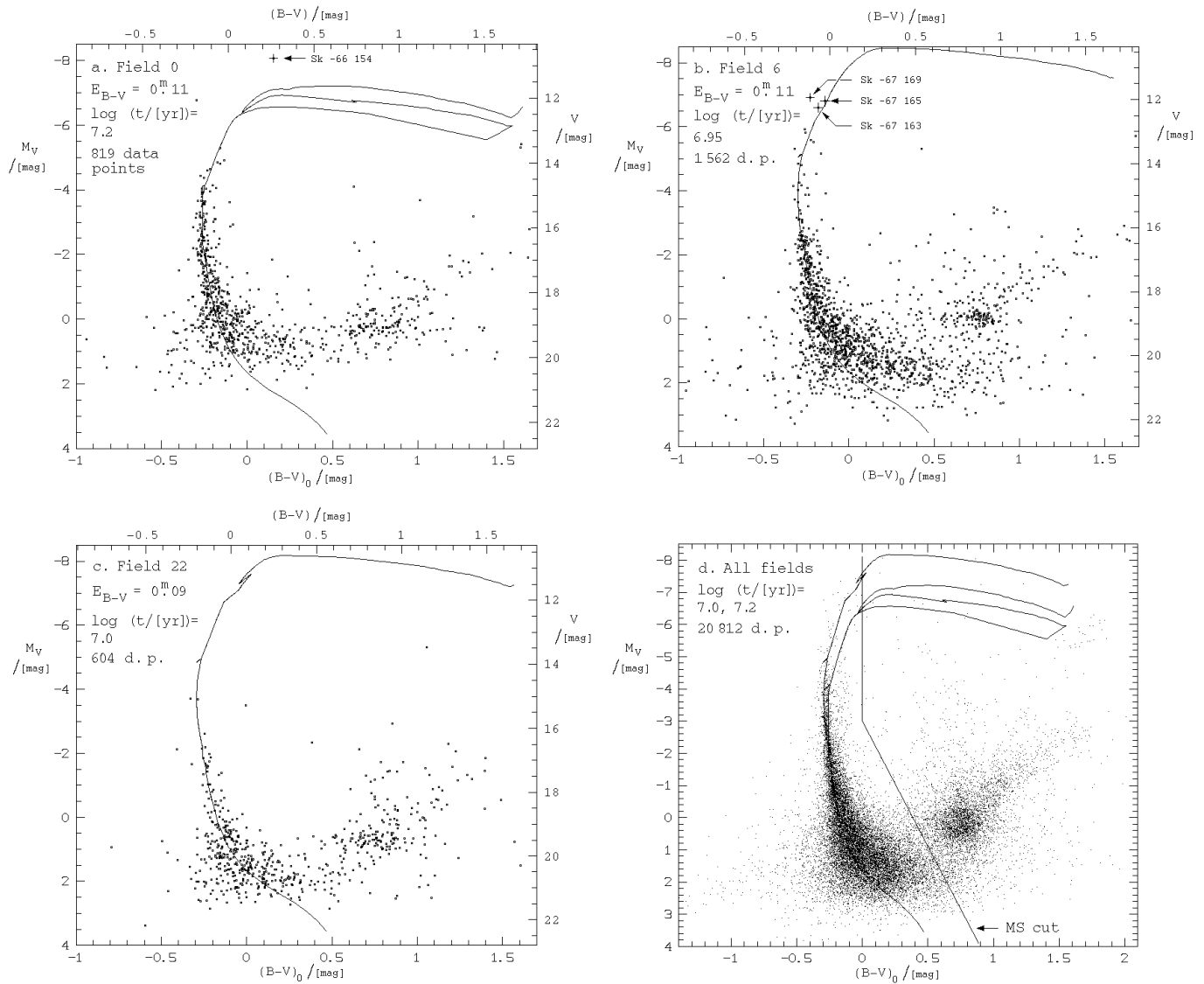


Fig. 2a–d. CMDs of the fields 0 (a), 6 (b) and 22 (c) with marked Sanduleak stars (1969) and of the whole analysed area (d) with the rough main sequence cut shown together with appropriate Geneva isochrones (Schaerer et al. 1993)

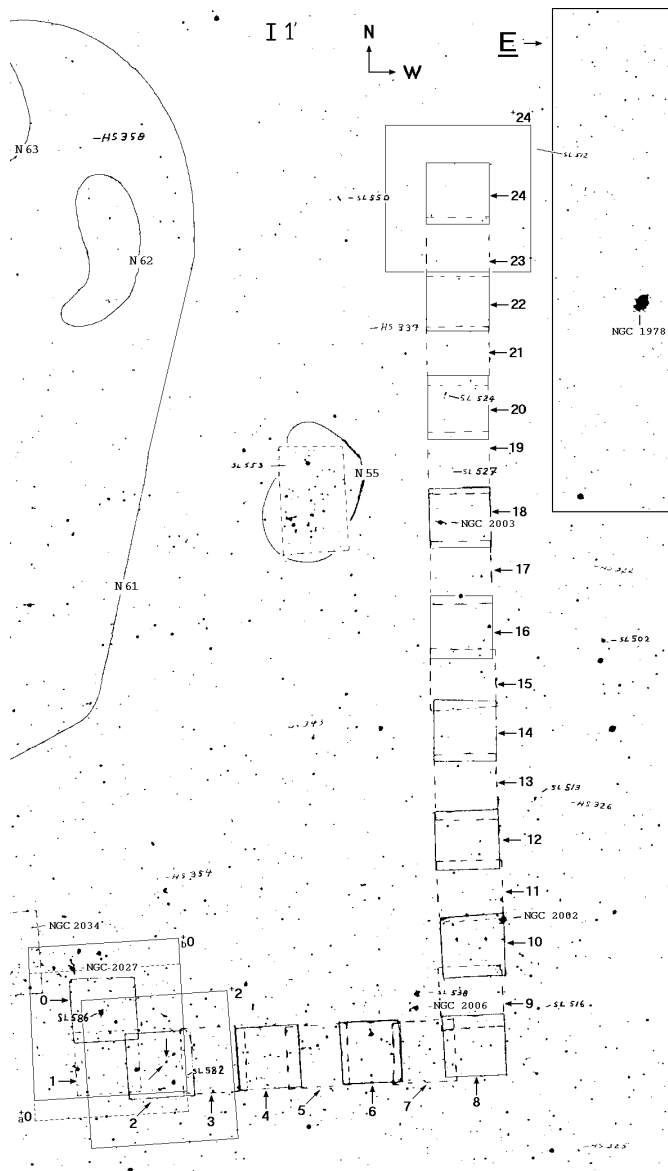


Fig. 3. Mosaic of the central region of LMC 4 out of 4 V charts (44, 45, 51, 52) of the LMC atlas of Hodge & Wright (1967). The 25 fields of the 1st dataset, the 3 fields of the 2nd dataset and the eastern part of key region E (de Boer et al. 1989, 1991) are outlined. In field 2 we marked Sk -67 198 (see Table 3) by two arrows

lute visual magnitude range for LMC objects of approximately $-6 \text{ mag} < M_V < 0 \text{ mag}$).

As examples of this fit to the 1st dataset we show four CMDs in Fig. 2: the CCD field 0 with the largest age of the analysed area (a), field 6 with one of the smallest ages (b), and field 22 to demonstrate the impossibility of fitting an isochrone to the last five fields (i.e. fields 20–24 corresponding to region e, see Sect. 4) because of a poorly populated upper main sequence (c). We also show the CMD for the whole 'J'-shaped region (i.e. all CCD fields, 0–24, without overlap) with the appropriate isochrones and the main sequence cut used to set up the mass

Table 4. Age (t), reddening (E_{B-V}) and number of stars ($N_{*,BV}$) of all 25 CCD fields of the 1st dataset containing 24 480 stars with B , V magnitudes (inclusive multiple counts for stars in the overlapping regions)

Region	Field	$N_{*,BV}$	t [Myr]	E_{B-V} [mag]
e	24	313	n	0.08
	23	368	n	0.08
	22	604	n	0.09
	21	819	n	0.10
	20	1 084	n	0.11
d	19	980	11	0.11
	18	1 132	11	0.11
	17	1 060	10	0.11
	16	1 067	10	0.09
	15	1 120	10	0.09
c	14	1 166	11	0.04
	13	698	11	0.00
	12	904	11	0.09
	11	998	11	0.11
	10	1 062	11	:0.11
b	9	1 286	14	:0.11
	8	1 582	13	:0.11
	7	1 746	10	:0.11
	6	1 562	9	:0.11
	5	1 625	9	:0.11
a	4	532	10	:0.11
	3	462	13	0.08
	2	813	13	0.11
	1	678	11	0.11
	0	819	16	0.11

'?' indicating rough values (see Sect. 3)

'n' number of MS stars too small for accurate age determination, but consistent with ~ 11 Myr

function (see Braun 1996 for all CMDs). We find that all our fields indicate an age between 9 and 16 Myr. The results of all 25 fields are listed in Table 4.

The top of the main sequence region may contain data points for evolved stars. Given the age derived we expect their number to be small so that they cannot effect the age determination in a significant way.

The values for the reddening are in accordance with the foreground reddening of $E_{B-V} \in [0.00; 0.15]$ mag (Oestreich et al. 1995). In performing the calibration of the fields in sequence from 3 to 11 we found small systematic inconsistencies. Since field 3 and 11 could be calibrated in an absolute manner, we have interpolated the calibration for the fields in between, leading to less certain values of the stellar colour and thus of E_{B-V} , as given in Table 4. We judge the effect of this uncertainty on the ages as negligible.

For all our fields one has to realize that we implicitly assume that all stars seen in a field belong to the same population. However, projection effects can mask age gradients, because in fitting isochrones one is only sensitive to the youngest star

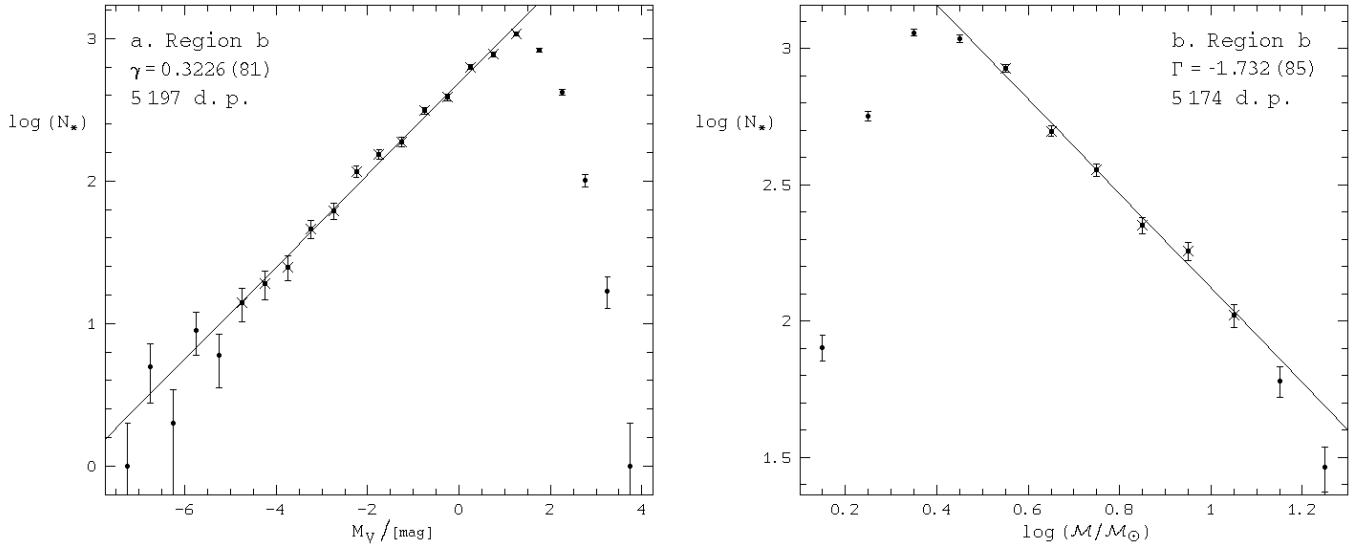


Fig. 4a and b. Luminosity (a) and mass function (b) of region b calculated from the Geneva isochrone (Schaerer et al. 1993) of $\log(t/[\text{yr}]) = 7.0$. The crosses mark the data points used in the fit (13 and 6 respectively)

population. Considering that star formation has been going on in all regions of the LMC some influence has to be expected. To handle this problem we investigate the luminosity and mass function for our region in the next section.

4. Luminosity function and mass function

To get a first hint about the possibility of a superposition of stellar populations with different ages - the isochrone fitting would only be sensitive for the youngest population if the turn-off points (TOPs) of the main sequence (MS) are not too different - we combine 5 CCD fields to one region (with an area of $59 \square'$ on the sky, see Fig. 1). For each region we construct the luminosity function (with slope γ) and the mass function (with slope Γ), as well as for the whole analysed area. This was made for equidistant intervals I with the usual approach (see Scalo 1986):

$$\log(N_{*,I_{M_V}}) = \gamma \cdot M_V/[\text{mag}] + \text{const.} \quad (3)$$

$$\log(N_{*,I_{\log(M/M_\odot)}}) = \Gamma \cdot \log(M/M_\odot) + \text{const.} \quad (4)$$

As an example we present in Fig. 4 the luminosity and the mass function of region b. The translation of brightness to mass for stars on the MS was done with the best fitting Geneva isochrone of 10 Myr, which can be described with the numerical relation:

$$M/M_\odot = 4.184 - 1.609 \cdot M_V/[\text{mag}] \quad (5)$$

$$+0.303 \cdot (M_V/[\text{mag}])^2$$

$$-0.036 \cdot (M_V/[\text{mag}])^3$$

$$-0.00094 \cdot (M_V/[\text{mag}])^4$$

$$+0.00173 \cdot (M_V/[\text{mag}])^5$$

Table 5. Per region the number of stars in the photometry is given. For the determination of the luminosity function with slope γ only the indicated number of stars on the main sequence is used. The same is given for the mass function (with the derived slope Γ). No correction for incompleteness at the faint end is made.

Region	$N_{*,BV}$	$N_{*,LF}$	γ	$N_{*,MF}$	Γ
e	2 794	2 031	0.406 (13)	2 031	-2.43 (5)
d	4 606	3 579	0.365 (09)	3 573	-2.12 (4)
c	4 151	3 102	0.303 (11)	3 039	-1.65 (9)
b	6 499	5 197	0.323 (08)	5 174	-1.73 (9)
a	2 762	2 129	0.220 (07)	2 118	-1.30 (8)
total J	20 812	16 038	0.318 (10)	15 986	-1.72 (4)

with a rms error of 0.031, being valid up to the TOP at $M_{V,\text{TOP}} = -4.93$ mag (corresponding to $M_{\text{TOP}} = 18.25 M_\odot$).

The resulting slopes are, as shown in Table 5, very close to the standard values of $\gamma \simeq 0.3$ and $\Gamma \simeq -1.35$ (Will 1996). A higher negative slope would indicate the superposition of different star populations (note that incompleteness in the faint bins causes a flatter distribution than it really would be).

Since the slopes we find are the same as those found in general, we conclude that there is no significant contribution of older age groups in these fields up to 300 Myr (equivalent to stars of $3 M_\odot$ still being on the main sequence). Even older star formation events may be present but they would contribute at fainter levels than the useable limit of our photometry.

5. The age of LMC 4

The ages of the various star groups of LMC 4 have been collected in Table 6. Note that the location of the various groups can be found in Fig. 1. For NGC 1948 we list only the newer

Table 6. Age (t) and reddening (E_{B-V}) of star populations in LMC 4 sorted from north to south, see Figs. 1 and 3

Object	t [Myr]	E_{B-V} [mag]	Paper
NGC 1978	2 200	0.08	Bomans et al. 1995
NGC 1948 ^a	5–10	0.20	Will et al. 1996
LH 72 ^b , north	8–15	0.00–0.04	Olsen et al. 1997
LH 72 ^b , south	5	0.06–0.17	Olsen et al. 1997
Region e ^c	n	0.08–0.11	this paper, Table 4
Region d ^c	10–11	0.09–0.11	this paper, Table 4
Region c ^c	11	0.00–:0.11	this paper, Table 4
Region b ^d	9–14	:0.11	this paper, Table 4
Region a ^d	10–16	0.08–:0.11	this paper, Table 4
NGC 2004	16	0.09	Sagar & Richtler 1991
LH 63 ^e	14	0.07	Petr 1994
LH 60 ^f	9	0.04	Petr 1994
LH 54 ^g	6	0.10	Petr 1994
LH 76 ^h	2–5	0.09	Wilcots et al. 1996

References for acronyms of LMC objects are:

LH . . . for one of the 122 OB associations and superassociations (Lucke & Hodge 1970),

N . . . for one of the 415 emission nebulae (Henize 1956),

DEML . . . for one of the 329 emission nebulae (Davies et al. 1976) and one of the 5 Shapley Constellations (McKibben Nail & Shapley 1953)

^a NGC 1948 - N 48 - DEML 189 - LH 52/53;

^b LH 72 - N 55 - DEML 228;

^c S–N strip - field 10–24 - region c–e;

^d E–W strip - field 0–9 - region a–b - LH 77 - main part of Shapley Constellation III;

^e LH 63 - NGC 1974 - N 51 A - DEML 201;

^f LH 60 - NGC 1968 - N 51 - DEML 201;

^g LH 54 - NGC 1955 - N 51 D - DEML 192;

^h LH 76 - NGC 2014 - N 57 A - DEML 229.

age determination of Will et al. (1996) superseding the one by Vallenari et al. (1993).

The ages we derived for the 'J'-shaped region are in the range of 9 to 16 Myr. Also NGC 1948, NGC 2004, LH 72 north, LH 63, and LH 60 are 9 to 16 Myr old. This seems to suggest that most of LMC 4 was formed as an entity some 9 to 16 Myr ago. Much younger are LH 54 and LH 76, with an age of 5 Myr, but these associations are located on the very rim of LMC 4.

N 51, with LH 63, 60 and 54, shows an age gradient (Petr et al. 1994; Petr 1994), a clear hint at SSPSF on smaller scales. Much more recent starformation was triggered at the edge of LMC 4, after the entire interior was in existence for some 5 Myr (the time between formation of the LMC 4 interior and that of LH 54). It is interesting to note that 5 Myr is about the time the more massive stars need to become supernova.

Also LH 72 south is young, but it may have formed indeed more recently, in the aftermath of events in LH 72 north.

Note that the globular cluster NGC 1978, the rather conspicuous object near the northern rim of LMC 4 and having an age of approximately 2 Gyr (Bomans et al. 1995), has nothing

to do with the creation and/or evolution of SGS LMC 4. This statement is valid for all objects older than 70 Myr.

Both NGC 1948 and NGC 1978 are part of the $30' \times 30'$ key region E centered at RA: $5^{\text{h}} 25^{\text{m}}$ and Dec: $-66^{\circ} 15'$ (de Boer et al. 1989, 1991; Will et al. 1995).

6. Toward the history of LMC 4

LMC 4 contains a substantial population of young stars of age 10 Myr, while a quite older (> 300 Myr) background population may exist. A huge gas cloud must have been present in which the conditions were favourable for the burst of star formation ~ 10 Myr ago. The consequences of that burst are observed today. These can be summarized as follows. A volume of which we see the projected surface area of about 1 kpc^2 is filled with essentially coeval stars. The volume contains little neutral gas in numerous low column density filaments (Domgörgen et al. 1995), and at the same time clearly contains ionized gas (see Bomans et al. 1996).

Inside LMC 4 we have a large number of young main sequence stars. From the present day mass function, extended with the same slope to the mass rich end to also include the original mass rich stars, we can calculate the number of stars in each mass range $[m_1; m_u]$ initially present in our 'J'-shaped region:

$$N_{*,J} = \int_{m_1}^{m_u} 10^{4.972(22)} \cdot (\mathcal{M}/\mathcal{M}_{\odot})^{-2.716(44)} d\mathcal{M} \quad (6)$$

A fit to the Geneva evolutionary tracks (Schaerer et al. 1993) for an initial mass $\mathcal{M} > 12 \mathcal{M}_{\odot}$ yields a stellar lifetime relation of:

$$t_* = (86 \pm 10) \text{ Myr} \cdot (\mathcal{M}/\mathcal{M}_{\odot})^{-0.722(62)} \quad (7)$$

Stars with an initial mass above $8 \mathcal{M}_{\odot}$ will become supernovae of Type II. Combining Eqs. (6) and (7) with $m_u = 125 \mathcal{M}_{\odot}$ we get the number of supernovae after a given time:

$$N_{*,J,SN}(t) \simeq 1.4 \cdot (t/[\text{Myr}])^{2.38} \quad (8)$$

For star populations one would expect all stars with $\mathcal{M} \in [18.3; 125] \mathcal{M}_{\odot}$ to have exploded into SNe in the first 10 Myr. Thus we get $N_{*,J,SN} = 320 \pm 30$, for roughly 5% of the LMC 4 area. Extrapolating from the 'J'-shaped region to the entire interior of LMC 4 means that in this SGS of 10 Myr age about $5\text{--}7 \cdot 10^3$ supernovae have exploded. With an average supernova energy output of 10^{51} erg the total number of past SNe will have dumped at least $10^{54.5}$ erg into LMC 4.

On the other hand, the supernova rate right after starformation is very small and Eq. (8) indicates that after 5 Myr only ~ 200 SNe have exploded inside LMC 4, or less than 10% of the total in 10 Myr.

At present there is little neutral gas inside LMC 4, whereas the structure must have had lots of relatively dense neutral gas for the star formation. We can estimate the minimum energy input required to dissolve the birth cloud. Assuming a thickness of originally 500 pc with a gas density n_{orig} in the volume V ,

the energy needed for total ionization is $V \cdot n_{\text{orig}} \cdot 13.6 \text{ eV} = n_{\text{orig}} \cdot 10^{53.5} \text{ erg cm}^3$. A further calculation shows that roughly $n_{\text{orig}} \cdot 10^{52} \text{ erg cm}^3$ can accelerate all particles of the entire birth cloud to 100 km s^{-1} , enough to disrupt the cloud. This energy is easily provided by the supernovae. In fact, a substantial fraction of the energy needed is already released between 5 and 8 Myr.

Summarizing, based on the recognition that all young stars of LMC 4 are nearly coeval at 10 Myr, and on the sequel that supernovae will go off everywhere inside LMC 4 at a fair rate dumping energy rather evenly in the birth cloud, we can explain the structure of LMC 4 as we see it today.

In consequence of that, once the first supernovae occur, their individual (but soon the collective) blast waves may trigger star formation at the edges. This fits with the age derived for LH 72 south. Starformation at the edges of LMC 4 will have taken place at very recent times as secondary process. We expect that an age determination for the stars in any of the H II regions to the east of LMC 4 will show very young ($< 5 \text{ Myr}$) ages, like the ones at the NW (Will et al. 1996) and the SW (Petr et al. 1994).

The present supernova rate inside LMC 4 as calculated from our equations is about 1 per 670 yr which is comparable to the SN rate of the whole LMC derived from counting supernova remnants (Chu & Kennicutt 1988). Our mass function and main sequence lifetime indicate an increase of the SN rate to 1 per 120 yr in 25 Myr from now, at a time when the stars of originally $8 M_{\odot}$ will explode.

7. Summary and conclusions

The ages found for the stars inside LMC 4 lie in the range of 9 Myr to 16 Myr without a visible correlation with the distance to the LMC 4 centre (see Table 4 and Fig. 3). This means that there must have been one triggering event for star formation inside the greatest SGS of the LMC with a diameter of 1.4 kpc, whereas at the rim of LMC 4 there is evidence for SSPSF (Petr et al. 1994; Petr 1994). Thus SSPSF can't be the creation mechanism of LMC 4 as claimed by the first models (see e.g. Dopita et al. 1985), even if one is able to find examples of SSPSF in this region on scales below 150 pc.

Acknowledgements. We thank Ger van Rossum for participation in the early stages of this project and organizing the observations of the 1st dataset. JMW thanks the ESO staff for their help in obtaining the 2nd dataset.

JMB, JMW and DJB acknowledge support from the Deutsche Forschungsgemeinschaft (DFG), in the frame of the Graduiertenkolleg "The Magellanic System and Other Dwarf Galaxies" (GRK 118/2-96). DJB is grateful for a Feodor-Lynen-Fellowship of the Alexander von Humboldt-Foundation.

We thank Antonella Vallenari for discussions, Martin Altmann for critically reading the manuscript and Rob Kennicutt for the scan used in Fig. 1.

References

Alongi M., Bertelli G., Bressan A., et al., 1993, A&AS 97, 851
Bomans D.J., Vallenari A., de Boer K.S., 1995, A&A 298, 427

Bomans D.J., de Boer K.S., Koornneef J., Grebel E.K., 1996, A&A 313, 101
Braun J.M., 1996, diploma thesis, University of Bonn
Burki G., Rufener F., Burnet M., et al., 1995a, A&AS 112, 383
Burki G., Rufener F., Burnet M., et al., 1995b, ESO Messenger 80, 34
Chu Y.-H., Kennicutt R.C., 1988, AJ 96, 1874
Davies R.D., Elliot K.H., Meaburn J., 1976, Mem. R. Astron. Soc. 81, 89 (DEM)
de Boer K.S., Azzopardi M., Baschek B., et al., 1989, ESO Messenger 57, 27
de Boer K.S., Spite F., François P., et al., 1991, ESO Messenger 66, 12
de Boer K.S., Tucholke H.-J., Seitter W.C., 1995, ESO Messenger 81, 20
Domgörgen H., Bomans D.J., de Boer K.S., 1995, A&A 296, 523
Dopita M.A., Mathewson D.S., Ford V.L., 1985, ApJ 297, 599
Feitzinger J.V., Glassgold A.E., Gerola H., Seiden P.E., 1981, A&A 98, 371
Goudis C., Meaburn J., 1978, A&A 68, 189
Henize K.G., 1956, ApJS 2, 315
Hodge P.W., Wright F.W., 1967, "The Large Magellanic Cloud", Smithsonian Press
Kennicutt R.C., Hodge P.W., 1986, ApJ 306, 130
Landolt A.U., 1992, AJ 104, 340
Lucke P.B., 1974, ApJS 28, 73
Lucke P.B., Hodge P.W., 1970, AJ 75, 171
McKibben Nail V., Shapley H., 1953, Proc. Nat. Acad. Sci. 39, 358
Meaburn J., 1980, MNRAS 192, 365
Oestreicher M.O., Goehermann J., Schmidt-Kaler T., 1995, A&AS 112, 495
Olsen K.A.G., Hodge P.W., Wilcots, E.M., Pastwick L., 1997, ApJ 475, 545
Petr M., 1994, diploma thesis, University of Bonn
Petr M., Bomans D.J., Grebel E.K., 1994, in the "3rd CTIO/ESO Workshop on the Local Group", Layden A., Smith R.C., Storm J.(eds.), ESO Conf. Proc. 51, p. 86
Ratnatunga K.U., Bahcall J.N., 1985, ApJS 59, 63
Reid N., Mould J., Thompson I., 1987, ApJ 323, 433
Rousseau J., Martin N., Prévot L., et al., 1978, A&AS 31, 243
Sagar R., Richtler T., 1991, A&A 250, 324
Sanduleak N., 1969, CTIO, Contribution No. 89
Scalo J.M., 1986, Fund. Cos. Phys. 11, 1
Schaerer D., Meynet G., Maeder A., Schaller G., 1993, A&AS 98, 523
Stetson P.B., 1987, PASP 99, 191
Tenorio-Tagle G., Bodenheimer P., 1988, ARA&A 26, 145
Tucholke H.-J., de Boer K.S., Seitter W.C., 1996, A&AS 119, 91
Vallenari A., Bomans D.J., de Boer K.S., 1993, A&A 268, 137
Westerlund B.E., 1990, A&AR 2, 29
Wilcots E.M., Hodge P.W., King N., 1996, ApJ 458, 580
Will J.-M., 1996, Ph.D. thesis, University of Bonn
Will J.-M., Bomans D.J., Tucholke H.-J., et al., 1995, A&AS 112, 367
Will J.-M., Bomans D.J., Vallenari A., Schmidt J.H.K., de Boer K.S., 1996, A&A 315, 125

This article was processed by the author using Springer-Verlag L^AT_EX A&A style file L-AA version 3.